

Interaction of Cytolytic Toxin CytB with a Supported Lipid Bilayer: Study Using an Acoustic Wave Device

Kathryn A. Melzak,[†] David J. Ellar,[‡] and Electra Gizeli^{*†,§}

Institute of Biotechnology, University of Cambridge, Tennis Court Road, Cambridge, United Kingdom, CB2 1QT, and Department of Biochemistry, University of Cambridge, 80 Tennis Court Road, Cambridge, United Kingdom, CB2 1QW

Received August 11, 2003. In Final Form: November 24, 2003

An acoustic technique was used to monitor the interaction of the pore-forming cytolytic toxin CytB with a positively charged supported lipid bilayer. The acoustic device, which is based on a waveguide geometry, is sensitive to changes in the mass of the supported bilayer. The specificity of the interaction, rate and extent of the association, reversibility and effect of previous depositions of toxin were investigated. The CytB was found to bind irreversibly to the lipids at all fractional coverages even when the protein-to-lipid ratio was high enough to imply that the protein was associating with the external surface of the bilayer. The CytB formed stable structures with the bilayer at high protein surface concentrations and did not appear to disrupt the bilayer in the manner of a detergent. The rate of association with the bilayer was found to be directly proportional to the solution concentration of CytB at higher concentrations but appeared to be low at a CytB solution concentration of 5 $\mu\text{g mL}^{-1}$, leading to relatively low amounts of CytB being associated with the bilayer.

Introduction

Pore-forming protein toxins are produced by a variety of pathogenic bacteria.¹ These proteins insert into the membranes of target cells, forming pores which permit the release of cell contents and can lead to cell death through lysis or other pathogenic effects.² Steps involved in pore formation include the initial association of the protein with the membrane surface, which may take place through interaction with a specific receptor, and the insertion into the hydrophobic portion of the lipid bilayer to form a membrane-spanning pore. Formation of oligomeric pores will also require an oligomerization step. Applications of protein toxins include their use as biological pesticides³ and selective permeabilizing agents for cell membranes.⁴

The δ -endotoxins are a heterogeneous family of proteins responsible for the most important insecticidal activities of *Bacillus thuringiensis*. The insecticidal specificity of different subspecies of *B. thuringiensis* depends on the toxin produced; although generally active against lepidopteran larvae, subspecies have also been isolated with activity against coleopteran⁵ and dipteran⁶ larvae

as well as against other orders of insects.⁷ The δ -endotoxins are produced by *B. thuringiensis* as inactive protoxins which form crystalline inclusions during sporulation. The protoxins are activated by proteases after solubilization in the midgut of susceptible insect larvae.⁸ Activated toxins can then insert into cell membranes of the midgut epithelial cells, leading to the eventual death of the insect larvae.⁹

The δ -endotoxins can be separated based on structural similarity into two groups, the Cry proteins and the cytolytic Cyt proteins. CytB is a member of the latter group, named because they can cause cytolysis of a variety of eukaryotic cells in vitro. CytB has a molecular weight of 29 236 and is known to form pores in liposomes containing lipids with unsaturated fatty acids.¹⁰ The structure of the CytB protoxin has been determined;¹¹ the monomer is composed of α -helices wrapped around a β -sheet. The initial binding of Cyt toxin is irreversible.¹² Oligomerization of CytB and the closely related CytA is thought to take place after association with the membrane¹³ to form a pore which may have a β -barrel structure.¹⁴ The diameter of the pore that is formed has been estimated to be 1–2 nm by following the movement of solutes with known size¹⁵ and with a stoichiometry of 4, 5, or 6.¹¹

* Corresponding author. E-mail: gizeli@imbb.forth.gr.

[†] Institute of Biotechnology.

[‡] Department of Biochemistry.

[§] Current address: Department of Biology, University of Crete and Institute of Molecular Biology and Biotechnology FORTH, P.O. Box 1527, Heraklion, Crete, Greece 71110.

(1) (a) Alouf, J. E.; Freer, J. H. *The Comprehensive Sourcebook of Bacterial Protein Toxins*; Academic Press: London, 1999. (b) Lesieur, C.; Vécsey-Semjén, B.; Abrami, L.; Fivaz, M.; Gisou van der Goot, F. *Mol. Membr. Biol.* **1997**, *14*, 45–64.

(2) Billington, S. J.; Jost, B. H.; Songer, J. G. *FEMS Microbiol. Lett.* **2000**, *182*, 197–205.

(3) (a) Höfte, H.; Whiley, H. R. *Microbiol. Rev.* **1989**, *53*, 242–255. (b) Van Frankenhuyzen, K. In *Bacillus thuringiensis, an Environmental Biopesticide: Theory and Practice*; Entwistle, P. F., Cory, J. S., Bailey, M. J., Higgs, S., Eds.; John Wiley: Chichester, 1993; pp 1–35.

(4) Bhakdi, S.; Weller, U.; Valev, I.; Martin, E.; Jonas, D.; Palmer, M. *Med. Microbiol. Immunol.* **1993**, *182*, 167–175.

(5) Krieg, V. A.; Huger, A. M.; Langenbruch, G. A.; Schmetter, W. Z. *Angew. Entomol.* **1983**, *96*, 500–508.

(6) Goldberg, L. J.; Margalit, J. *Mosquito News* **1977**, *37*, 355–358.

(7) Drummond, J.; Miller, D. K.; Pinnock, D. E. *J. Invertebr. Pathol.* **1992**, *60*, 102–103.

(8) Lüthy, P.; Cordier, J.-L.; Fischer, H.-M. In *Bacillus thuringiensis as a Bacterial Insecticide: Basic Considerations and Applications*; Kurstak, E., Ed.; Marcel Dekker: New York, 1982; pp 35–74.

(9) Ellar, D. J.; Knowles, B. H.; Carroll, J.; Horsnell, J.; Haider, M. Z.; Ahmad, W.; Nicholls, C. N.; Armstrong, G.; Hodgman, C. In *Genetics and Biochemical Studies of the Mechanism of Action of Bacillus thuringiensis Entomocidal Endotoxins*; Rappouli, R., Alouf, J., Freer, J., Fehrenbach, F., Wadstrom, T., Witholt, B., Eds.; Gustav Fischer Verlag: Stuttgart, 1989; pp 499–506.

(10) Thomas, W. E.; Ellar, D. J. *FEBS Lett.* **1983**, *154*, 362–368.

(11) Li, J.; Koni, P. A.; Ellar, D. J. *J. Mol. Biol.* **1996**, *257*, 129–152.

(12) Chow, E.; Singh, F. J. P.; Gill, S. S. *Appl. Environ. Microbiol.* **1989**, *55*, 2779–2788.

(13) CytA: (a) Maddrell, S. H. P.; Lane, N. J.; Harrison, J. B.; Overton, J. A.; Moreton, R. B. *J. Cell. Sci.* **1988**, *90*, 131–144. CytB: (b) Promdonkoy, B. Ph.D. Thesis, University of Cambridge, Cambridge, U.K., 1999.

(14) Du, J.; Knowles, B. H.; Li, J.; Ellar, D. J. *Biochem. J.* **1999**, *338*, 185–193.

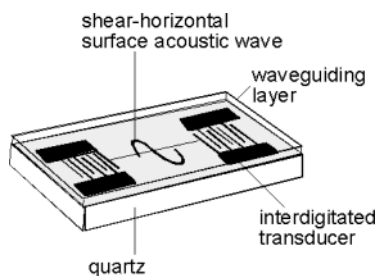


Figure 1. Schematic representation of the acoustic waveguide device. An acoustic wave can be generated by application of an alternating current across the two large contact pads of one of the interdigitated transducers; the wave propagates across the device surface before being converted back to an electrical signal. A dielectric layer deposited on the device surface is used to guide the wave close to the sensing surface. Note that the bars on the transducers are not drawn to scale.

Experimental approaches used to derive information on the mechanism of pore-forming toxins such as CytB include structural studies based on techniques such as proteolysis, fluorescence experiments, and amino acid substitutions. The above techniques are solution-based; the native or mutant toxin is applied to a suspension of cells or vesicles, and the effect of the toxin is tested after an incubation period. The development of methods for the formation of robust model membrane structures at solid/liquid interfaces¹⁶ has allowed the real-time study of membrane interactions using biosensors. As a result, optical,¹⁷ electrochemical,¹⁸ and acoustic¹⁹ devices have been used in combination with supported lipid bilayers as a powerful technique to study membrane events and provide quantitative information on the kinetic and binding constants of interactions.

Acoustic devices have been shown to be an attractive alternative to optical techniques for label-free, real-time monitoring of protein and cellular interactions.²⁰ In the work presented here, a high-frequency acoustic sensor is used to monitor association of the pore-forming CytB toxin with a supported bilayer. The real-time monitoring facilitates kinetic measurements; the rate of association can be determined as a function of solution and surface concentration of protein, and the irreversible nature of the association can be readily determined.

Principles of Acoustic Measurements

The acoustic wave device used in this study is based on a waveguide geometry consisting of a high-frequency (108 MHz) surface acoustic wave (SAW) device overlaid by a thin waveguide (Figure 1). The waveguide should be an elastic material²¹ and must have a shear velocity lower than that of the substrate. Acoustic waves can be generated and detected on the surface of a SAW device by using a

set of interdigitated transducers (IDTs) deposited on a piezoelectric substrate as shown in Figure 1. The cut of the piezoelectric substrate (quartz) used in this application results in generation of a shear wave that propagates inside the bulk and on the surface of the device. The addition of a thin waveguide consisting of polymer or silica to the device surface improves the efficiency of transmission of the shear wave by guiding the acoustic energy at the surface of the device. The acoustic wave that travels in the above geometry is known as the Love wave, and the device as the acoustic waveguide or Love wave device.²² The efficiency and speed of transmission of the acoustic wave are affected by changes occurring on the sensing surface between the IDTs and can therefore be monitored to follow changes resulting from the adsorption of mass. More information on the waveguide geometry and the effect of the overlayer thickness on acoustic wave-guiding can be found in the literature.²³ Of the available acoustic wave sensors, the acoustic waveguide device has been shown to exhibit the highest mass sensitivity.²⁴

The Love wave is a shear wave, which means that application of liquid to the device surface does not damp the wave excessively and the device can operate effectively in liquid environments. Liquid in contact with the device will exhibit viscous coupling to the oscillating surface, with the oscillations being carried out into the solution to a penetration depth determined by the viscosity and density of the liquid and the frequency of the oscillation.^{24a} The thickness δ of the entrained fluid layer is given by

$$\delta = \sqrt{\frac{2\eta}{\rho\omega}} \quad (1)$$

where η is the solution viscosity, ρ is the density, and ω is the oscillation frequency. At the 104 MHz operating frequency of the devices used in these experiments, the thickness of the entrained layer for a device operating in water is approximately 56 nm. Transmission of the acoustic wave in water will therefore be affected by changes in the density and viscosity occurring within 56 nm of the device surface. A change in the surface charge density can also affect the transmission of the acoustic wave; this is because the compression of the piezoelectric quartz substrate is accompanied by a change in dipole moment so that there will be an oscillating electric field on the device surface as well as an acoustic wave.

The speed of the wave, measured as phase change, has been modeled and experimentally demonstrated for the acoustic waveguide device as being proportional to mass bound at the device surface for thin elastic mass layers.²⁵ Phase measurements were monitored during the following experiments and used to follow binding of protein to the supported bilayer on the device surface. Changes due to acousto-electric interactions are considered to be minimal and, therefore, not taken into account.

Experimental Procedures

Purification of CytB. CytB was purified in the form of crystal inclusions from strains of recombinant *B. thuringiensis* IPS78/

(15) Drobniowski, F. A.; Ellar, D. J. *Curr. Microbiol.* **1988**, *16*, 195–199.

(16) Heyse, S.; Stora, T.; Schmid, E.; Lakey, J.; Vogel, H. *Biochim. Biophys. Acta* **1998**, *1376*, 319–338.

(17) Bieri, C.; Ernst, O. P.; Heyse, S.; Hofmann, K. P.; Vogel, H. *Nat. Biotechnol.* **1999**, *17*, 1105–1108.

(18) Cornell, B. A.; Braach-Maksyvytis, V. L. B.; King, L. G.; Osman, P. D. J.; Raguse, B.; Wiczorek, L.; Pace, R. J. *Nat. Biotechnol.* **1997**, *387*, 580–583.

(19) Gizeli, E.; Liley, M.; Lowe, C. R.; Vogel, H. *Anal. Chem.* **1997**, *69*, 4808–4813.

(20) Several different designs of acoustic sensors operate in liquids. Applications of the commercially available low-frequency quartz crystal resonators are reviewed in: (a) Janshoff, A.; Galla, H.-J.; Steinem, C. *Angew. Chem., Int. Ed.* **2000**, *39*, 4004–4032. The high-frequency waveguide device used here is described in: (b) Caliendo, C.; D'Amico, A.; Verardi, P.; Venema, W. *IEEE Ultrason. Symp. Proc.* **1990**, 383.

(21) Wang, Z.; Cheeke, J. D. N.; Jen, C. K. *Appl. Phys. Lett.* **1994**, *64*, 2940–2942.

(22) Love waves are named for A. E. H. Love. Mathematical analysis of Love waves is reviewed extensively in the literature on seismology.

(23) (a) Du, J.; Harding, G. L.; Ogilvy, J. A.; Dencher, P. R.; Lake, M. *Sens. Actuators, A* **1996**, *56*, 211–219. (b) Gizeli, E.; Goddard, N. J.; Lowe, C. R.; Stevenson, A. C. *Sens. Actuators, B* **1992**, *6*, 131–137.

(24) (a) Ballantine, D. S.; White, R. M.; Martin, S. J.; Ricco, A. J.; Zellers, E. T.; Frye, G. C.; Wohltjen, H. *Acoustic Wave Sensors*; Academic Press: San Diego, 1997. (b) Kovacs, G.; Venema, A. *Appl. Phys. Lett.* **1992**, *61*, 639–641.

(25) McHale, G.; Newton, M. I.; Martin, F. *J. Appl. Phys.* **2002**, *91*, 9701–9710.

11²⁶ containing the chloramphenicol-resistant plasmid pBYCYTB by sucrose density gradient ultracentrifugation.²⁷ The cytolitic toxin inclusions were kept in distilled water at $-20\text{ }^{\circ}\text{C}$ at $1\text{--}10\text{ mg mL}^{-1}$ and were solubilized in the appropriate buffer before use. The activity of CytB was confirmed by a hemolysis assay.²⁸

Acoustic Devices. The acoustic devices were prepared by photolithography at the Southampton Electronics Centre (Southampton, U.K.) using single-crystal Y-cut, z-propagating 0.5 mm thick quartz, with a 200 nm gold overlayer and a 10 nm chromium adhesion layer. The input and output IDTs produced by the photolithographic patterning consisted of 40 pairs of split fingers with a periodicity of $45\text{ }\mu\text{m}$; the wavelength of the acoustic wave was therefore $45\text{ }\mu\text{m}$, and the operating frequency of the uncoated device was 108 MHz. A $1.2\text{ }\mu\text{m}$ thick waveguide layer of poly(methyl methacrylate) (PMMA) was deposited on the surface of the acoustic device by spin-coating the device at 4000 rpm with a 22% solution of medium molecular weight PMMA (Aldrich) in 2-ethoxyethyl acetate (Aldrich).¹⁹ The PMMA-covered devices were heated to $195\text{ }^{\circ}\text{C}$ for 2 h to facilitate solvent evaporation. The operating frequency of the acoustic waveguide device was 104 MHz.

Instrumentation and Experimental Setup for Acoustic Experiments. A Hewlett-Packard 4195A network analyzer was used to measure the amplitude and phase of the output electrical signal with respect to a reference signal. Data were collected on a PC using LabView software. A Perspex flow cell with a silicone rubber gasket was used to hold the solution in place over the region of the device between the IDTs, exposing an area of approximately 0.12 cm^2 . During experiments, a 3 MHz region of the frequency spectrum near the maximum operating frequency was scanned every 43 s to monitor the signal. Data were collected at a fixed frequency so that one data point was collected every 43 s. Experiments were carried out at ambient temperature. The phase change is normalized to 0 at the start of the experiments so that the value plotted indicates the relative change over the course of each experiment.

Modification of the PMMA-Coated Devices with a Silicate Layer. A silicate gel was prepared by condensation from tetraethyl orthosilicate (TEOS, from Aldrich) in the presence of acid.²⁹ To produce a smooth layer, the TEOS was hydrolyzed in acid by placing 0.05 g of TEOS in a 1.5 mL microcentrifuge tube and adding 5.8 M HCl to give a final volume of 1 mL. The tube was vortexed for 30 s or until only one liquid phase was visible. To form smooth layers, the PMMA-coated device was spin-coated with an initial layer of TEOS: 5 drops of TEOS was left on the surface for 5 s before spinning at 4000 rpm for 40 s. The hydrolyzed TEOS was added to the device surface between 3 and 4 min after the end of the vortexing and left on the device surface for 30 s before spin-coating as before for 40 s at 4000 rpm. The device surface was rinsed with water approximately 2 min after the end of the spin-coating. The rougher silicate layers, with a peak-to-trough height in the range of 25 nm ,²⁹ were prepared using a silicate gel made from 0.25 g of TEOS made up to 1 mL with 5.8 M HCl. The gel was left for 30 min at room temperature and then placed on the PMMA-coated device for 2 min before being rinsed off with water.

Preparation of Lipid Vesicles for Acoustic Experiments. Unilamellar lipid vesicles were prepared by extrusion using an Avestin Liposfast Basic extrusion apparatus. Vesicles were made from 2-oleoyl-1-palmitoyl-*sn*-glycero-3-phosphocholine (POPC, Fluka), cholesterol (chol, Sigma), and stearylamine (Sigma).¹⁴ The POPC, cholesterol, and stearylamine were used at a mole ratio of 4:3:1 for CytB binding studies. Stock solutions of lipids were made up in chloroform and mixed to give the appropriate mole ratio. The chloroform was removed by evaporation under nitrogen for 1 h. Care was taken to maintain the solution at room temperature during the evaporation in order to prevent precipitation of the stearylamine. The dried lipids were resuspended

in phosphate-buffered saline (PBS) (0.01 M phosphate, 0.0027 M KCl, and 0.137 M NaCl at pH 7.4; tablets from Sigma) at a total lipid concentration of 2 mg/mL and then extruded 21 times through a 50 nm pore membrane (Avestin).

Glucose Release Assay. Vesicles with entrapped glucose were prepared as described above but with POPC, cholesterol, and stearylamine resuspended and extruded in PBS with added glucose. The vesicles were transferred into PBS with no glucose using Sephadex G-50.¹⁴ Five milliliters of preswelled G-50 was added to the barrel of a 5 mL syringe. This was centrifuged at 2000 rpm using a swinging bucket rotor to leave a column of dry gel bed. Liposomes extruded in glucose were applied to the top of the column which was then centrifuged and rinsed with buffer. Liposomes with entrapped glucose eluted from the column and were used for glucose release assays.¹⁴ Liposomes were incubated with CytB at room temperature; the amount of glucose released from the liposomes was determined at the end of the incubation period using a hexokinase assay.³⁰ Triton X-100 at 1% was added to obtain 100% release of glucose. The release of glucose is a measure of pore formation on the vesicles.³⁰

CytB Association with Vesicles. Liposomes were incubated at room temperature with CytB or bovine serum albumin (BSA). The liposomes and associated protein were pelleted by centrifugation at 13 000 rpm in a microcentrifuge for 10 min. Pellets were washed with buffer twice; samples from the pellets and supernatants were then analyzed using Tris/glycine SDS-PAGE.¹⁴

Formation of Supported Lipid Bilayer. Lipid bilayers were prepared by spontaneous fusion of liposomes on the surface of the modified acoustic device. Acoustic devices modified in the way described here have been shown previously to be suitable for formation of bilayers in this way.²⁹ A continuous flow of PBS was pumped over the surface of the modified acoustic devices at a rate of 0.083 mL min^{-1} using a peristaltic pump. Vesicle suspensions at a concentration of 0.02 mg mL^{-1} total lipid content were run over the surface of the device for 15 min. The device was then rinsed with PBS until the acoustic signal had reached a steady state. The presence of a bilayer as opposed to a layer of adsorbed vesicles is associated with a characteristic change in the acoustic signal.^{29,31} Lipid bilayers could be rinsed off the surface with 0.1% w/v Triton X-100 (Fisher) in PBS.

Addition of CytB to a Supported Lipid Bilayer (SLB). Samples of various concentrations of CytB in PBS were added to the SLB-modified device surface under continuous flow (0.083 mL min^{-1}). The toxin solution was pumped over the bilayer for a limited time, which was either (2×43) s, the time required to collect two data points, or (8×43) s, the time required to collect eight data points. In addition to CytB, BSA (Sigma) and cytochrome *c* (Sigma) were also added to the SLB for (2×43) s. After addition of the protein, the PBS rinsing was resumed until the signal had again reached a steady state.

Results and Discussion

Formation of a Supported Lipid Bilayer. The vesicle fusion technique has been applied by many researchers to form supported lipid bilayers.³² This convenient method can be used in combination with a flow-through cell to deposit bilayers on smooth hydrophilic surfaces; the surfaces can be regenerated by addition of detergent so that successive rounds of fresh bilayer can be deposited during the course of one experiment. Formation of SLBs by vesicle fusion has the further advantage of leaving an aqueous layer between the lipids and the underlying substrate which leads to a better model for cell membranes than that formed by hybrid bilayers in which one monolayer is directly attached to the substrate surface.

(26) Ward, E. S.; Ellar, D. J. *FEBS Lett.* **1983**, *158*, 45–49.

(27) Knowles, B. H.; White, P. J.; Nicholls, C. N.; Ellar, D. J. *Proc. R. Soc. London, Ser. B* **1992**, *114*, 415–420.

(28) Thomas, W. E.; Ellar, D. J. *J. Cell Sci.* **1983**, *60*, 181–197.

(29) Melzak, K.; Gizeli, E. *J. Colloid Interface Sci.* **2002**, *264*, 21–28; this reference shows AFM images of the rough and smooth silicate surfaces. Roughness on the scale of the vesicle size interferes with deposition of bilayers.

(30) Kinsky, S. C. *Methods Enzymol.* **1974**, *32*, 501–513.

(31) Keller, C. A.; Kasemo, B. *Biophys. J.* **1998**, *75*, 1397–1402.

(32) (a) Csucs, G.; Ramsden, J. J. *Biochim. Biophys. Acta* **1998**, *1369*, 61–70; in this paper, the mass of POPC bilayers is calculated to be 350 ng cm^{-2} at a surface pressure of 32 mN m^{-1} , close to the value of 330 ng cm^{-2} that was observed by SPR. (b) Liley, M.; Bouvier, J.; Vogel, H. *J. Colloid Interface Sci.* **1997**, *194*, 53–58. (c) Nollert, P.; Kiefer, H.; Jaehning, F. *Biophys. J.* **1995**, *69*, 1447–1455.

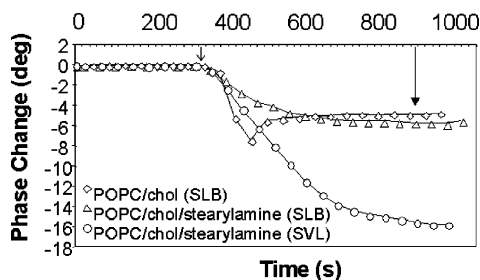


Figure 2. Change of the acoustic signal during the application of a vesicle suspension of POPC/cholesterol (diamonds) and POPC/chol/stearylamine (triangles) to a smooth silicate surface and of POPC/chol/stearylamine (circles) to a rough silicate surface; the first two resulted in the formation of a supported lipid bilayer while the third resulted in a supported vesicle layer. The open arrow indicates the start of vesicle deposition, and the closed arrow indicates the start of the buffer rinse.

The lipid layer formed after application of vesicles to the surface must be analyzed to distinguish single bilayers from multilayers or adsorbed vesicle layers and also to determine the extent of defects in the bilayer. The modified surface used here has been shown previously to be suitable for formation of bilayers.²⁹ One of the advantages of acoustic measurements is that they can be used to monitor formation of a bilayer and to distinguish between bilayers and adsorbed vesicle layers. This has been confirmed previously by separate research groups using two different acoustic techniques;^{29,31} the presence of bilayers as indicated by the acoustic measurements was confirmed by fluorescence recovery after photobleaching of labeled lipids to demonstrate the lateral diffusion that is indicative of bilayer presence and by using ¹⁴C labeled lipids or other methods to determine the amount of lipids present on the surface.

Surface plasmon resonance (SPR) experiments used to calibrate the phase change measured by the acoustic device have shown that 1° phase change corresponds to adsorption of a protein layer with a surface density of 65 ± 6 ng cm⁻². If this number is used to determine the amount of lipid on the device surface after formation of the positively charged SLBs used here, the $5.0 \pm 0.6^\circ$ ³³ phase change detected (Figure 2) would correspond to a surface concentration of 325 ng cm⁻², slightly lower than some previously measured values^{32a} but in good agreement with the values accepted for bilayers.^{32d} Microscope images of fluorescently labeled bilayers show continuous coverage of the surface, indicating that there are no bare patches on the surface.²⁹ Addition of BSA to the positively charged bilayer (Figure 3) resulted in no significant change in signal; since BSA binds to defects in the bilayer,³⁴ these results imply formation of a bilayer with few defects.

Figure 2 also shows the phase response for deposition of positively charged and neutral SLBs, indicating that the surface charge does not have a significant effect on the net change in signal. The phase response is also shown for deposition of a vesicle layer on a rough silicate surface. The kinetics of formation of the positively charged SLB differs from that for forming the neutral SLB; the initial dip^{29,31} in the signal is not present, as if fewer vesicles adsorb prior to fusing to form the SLB. This may be due to faster fusion of the positively charged vesicles as a result

(33) Different waveguide devices exhibit slightly different sensitivities. Although all experiments were performed multiple times and on various devices, data reported here were obtained on the same 104 MHz device and whenever possible during the same experiment.

(34) Cevc, C.; Strohmaier, L.; Berkholz, J.; Blume, G. *Stud. Biophys.* **1990**, *138*, 57–70.

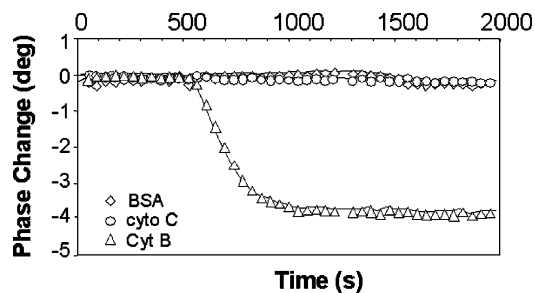


Figure 3. Real-time phase change detected during the addition of one aliquot of $20 \mu\text{g mL}^{-1}$ of BSA, cytochrome *c*, and CytB for (2×43) s on a POPC/chol/stearylamine SLB.

of electrostatic attraction with the silicate surface, which will be negatively charged.³⁵

Control Experiments. The specificity of the binding of CytB to a positively charged SLB was investigated by applying other proteins to the lipid bilayer; each protein sample was added for 2×43 s followed by a buffer rinse. It can be seen in Figure 3 that only the CytB causes a significant change in the acoustic signal. At the pH of 7.4 used in these experiments, the CytB, with a pI of 5.2, will be negatively charged. Control experiments with CytB added to a SLB with POPC and cholesterol but no stearylamine showed a phase change that was approximately 75% smaller than that observed with the positively charged bilayer, indicating that there is a strong electrostatic component to the binding. Electrostatic attraction is not in itself sufficient to cause the interaction with the bilayer that is observed here; addition of BSA, with a pI of 4.2, resulted in almost no change to the acoustic signal (Figure 3). Application of CytB directly to the silicate-modified acoustic device resulted in no change in the acoustic signal.

The oleoyl group of the POPC provided the unsaturated fatty acid required for CytB insertion into the bilayer, and cholesterol was added to model eukaryotic membranes. Stearylamine was added to be able to make comparisons to other *in vitro* studies¹⁴ and increase the interaction of CytB with the bilayer so that the conditions giving optimum binding could be characterized.

Glucose release assays showed that the CytB formed pores in vesicles with the lipid composition used here releasing all of the glucose, as expected.¹⁴

The SDS-PAGE analysis of protein association with the positively charged liposomes showed that incubation of CytB at a protein-to-lipid weight ratio of 1:4 resulted in the protein associating entirely with the pelleted fraction, with no protein remaining in the supernatant (data not shown). Incubation of CytB with liposomes at a weight ratio of 1:2 resulted in some CytB in the supernatant, although the majority of the protein remained associated with the liposome pellet. Incubation of liposomes with BSA at the same weight ratio (1:2) resulted in the BSA remaining predominantly in the supernatant. These results show that CytB can associate with the positively charged liposomes at very high protein-to-lipid ratios.

CytB Binding Kinetics. The interaction of CytB with the SLB was found to be irreversible under the conditions used here, with no reversal of the drop in phase observed after extensive buffer rinsing (Figure 3). For irreversible interaction of CytB with the bilayer, the flux of CytB at the surface of the bilayer is equal to the product of the association constant k_a and the concentration of CytB

(35) Melzak, K. A.; Janzen, J.; Brooks, D. E. *J. Colloid Interface Sci.* **1995**, *174*, 480–489.

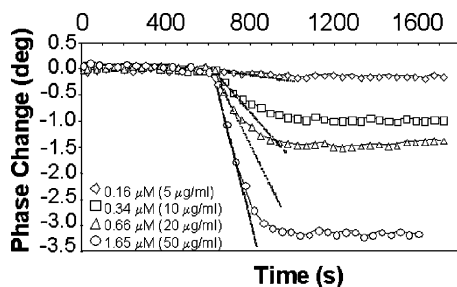


Figure 4. Phase change as a function of time during the application of four different concentrations of CytB to a SLB; each concentration was left for (2×43) s, the time required to obtain two data points, followed by buffer rinse.

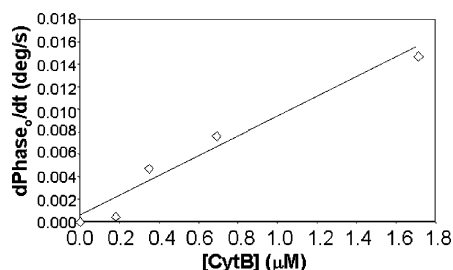


Figure 5. Plot of the rate of phase change measured from Figure 3, where ΔPhase_0 corresponds to the phase change measured during the first (43×2) s after toxin addition, as a function of CytB concentration. The line, fitted by using linear regression analysis, corresponds to a slope of $0.88 \times 10^4 \text{ deg M}^{-1} \text{ s}^{-1}$ and $R^2 = 0.969$.

adjacent to the surface.³⁶ The association k_a is the apparent first-order association constant in cm s^{-1} . This equation is satisfied at low surface concentrations of CytB, where the rate of interaction is not limited by available binding sites on the bilayer. The value k_a can be determined by plotting the change in surface concentration of the bilayer-associated CytB as a function of solution CytB concentration. If the value for the initial rate of association of CytB with the bilayer is used, this will satisfy the requirement for low surface concentrations. In these experiments at any given time, the acoustic phase is considered as being proportional to mass, so that the change in phase is proportional to the mass of the membrane-associated CytB.

Different concentrations of CytB were applied to the SLB-modified device for 2×43 s, resulting in the acoustic responses shown in Figure 4. To estimate the initial reaction rate, $d\text{Phase}_0/dt$, the phase change measured over the first 86 s is fitted to a straight line for each CytB concentration applied. The slopes of the initial-rate-line fits are plotted in Figure 5 as a function of solution concentration of CytB. Linear regression of all data in Figure 5, that is, from 0.16 to $1.65 \mu\text{M}$ (5 to $50 \mu\text{g mL}^{-1}$, respectively), yielded a fit with a slope of $0.88 \times 10^4 \text{ deg M}^{-1} \text{ s}^{-1}$, ($R^2 = 0.96$) corresponding to a k_a of $1.95 \times 10^{-5} \text{ cm s}^{-1}$. Linear regression is used here for the analysis although the association seems to be lower at $5 \mu\text{g mL}^{-1}$; values of the phase change observed at $5 \mu\text{g mL}^{-1}$ are too low to be able to measure a separate rate association constant over the concentration range of 0 – $5 \mu\text{g mL}^{-1}$. The concentration dependence of the CytB binding is discussed further in the section on addition of multiple aliquots. If concentrations of $10 \mu\text{g mL}^{-1}$ or higher only are used in the regression analysis, the value obtained for the rate constant decreases from 1.95×10^{-5} to 1.6×10^{-5}

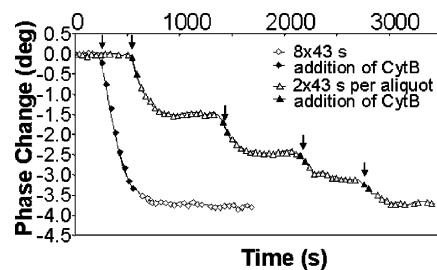


Figure 6. Comparison of the phase change as a function of time during the addition of $20 \mu\text{g mL}^{-1}$ of CytB as one aliquot for (8×43) s and four aliquots for (2×43) s per aliquot. The time at which the protein reached the surface is indicated by an arrow, and the points that correspond to the time that CytB was in contact with the SLB are indicated by filled circles or triangles.

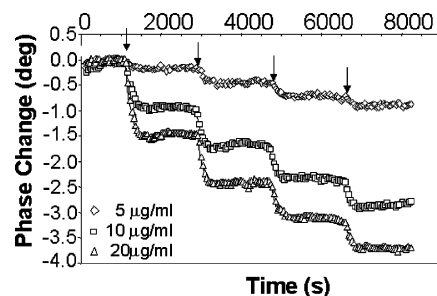


Figure 7. Phase change in real time during the sequential addition of four aliquots of 5, 10, and $20 \mu\text{g mL}^{-1}$ of CytB, each one applied for (2×43) s; the arrows correspond to the time at which each aliquot was applied.

cm s^{-1} . The values obtained here for the association rates are within the range observed previously for protein adsorption to surfaces.³⁶

Association of proteins with surfaces can be limited by the reaction at the surface, by mass transport from solution, or by a combination of the two. One way to determine which is the limiting factor is to calculate the mass transport coefficient and compare it to the measured association constant to see which value is smaller. The mass transfer coefficient for CytB in the flow conditions used here was calculated to be $2.6 \times 10^{-4} \text{ cm s}^{-1}$;³⁷ this is larger than the measured association constant, implying that mass transport is not the limiting factor and that the association measured here is the interaction of CytB with the SLB.

Addition of Sequential Aliquots of CytB. Samples at $20 \mu\text{g mL}^{-1}$ of Cyt B were applied to a SLB deposited on the device surface either as a single aliquot over a total period of (8×43) s or as a sequence of four aliquots over a period of (2×43) s each per aliquot (Figure 6). The total phase drop observed after the addition of four aliquots was found to be 3.7° ; this is the same as the phase drop detected after the addition of one single aliquot of $20 \mu\text{g mL}^{-1}$ of CytB for the same total time period. Four aliquots of 5 and $10 \mu\text{g mL}^{-1}$ of CytB were also applied to a SLB formed on the device surface in a way similar to that shown in Figure 6 for the $20 \mu\text{g mL}^{-1}$ sample, that is, for a period of (2×43) s per aliquot. Figure 7 shows the phase change observed for the three concentrations.

The minimum surface concentration of CytB detected in association with the POPC/chol/stearylamine bilayer was 6.8 ng cm^{-2} , calculated from the phase change after the addition of the first aliquot of CytB at $5 \mu\text{g mL}^{-1}$ (Figure 7). The maximum surface concentration detected from

(36) Slack, S. M.; Horbett, T. A. *J. Colloid Interface Sci.* **1989**, *133*, 148–165.

(37) Additional information is available on the calculation of the mass transfer coefficient.

Figure 6 was 240 ng cm^{-2} , or 0.7 g per g of lipid on the surface. If an area per molecule of $33.5 \text{ \AA} \times 85 \text{ \AA}$ is assumed for the CytB molecule,¹¹ the maximum surface concentration of CytB corresponds to an area of $1.4\times$ that of a monolayer of protein. This leads to some questions with regard to the arrangement of the proteins and the lipids; there is sufficient lipid to cover the surface with a bilayer and sufficient CytB to cover the surface with an additional layer of protein. Insertion into the lipid bilayer does not account for the surface concentration of protein observed here, even if no lipid is displaced into the solution. The CytB therefore seems to form an adsorbed layer on the surface of the bilayer. One way to obtain the high concentrations observed here would be if the CytB oligomerized on the external surface of the bilayer.

The CytA protein, which differs from CytB by a 15 aa C-terminal extension, associates with vesicles at high protein-to-lipid ratios before causing release of solutes; this is thought to suggest a detergent-like mechanism.³⁸ The results obtained here indicate that CytB does not disrupt the bilayer even at high concentrations: extensive rinsing after addition of CytB to SLBs does not result in desorption of mass, implying that the CytB forms a stable structure with the SLB rather than breaking the SLB apart in a detergent-like manner.

Figures 6 and 7 show that the binding of CytB is irreversible, even when the SLB is becoming saturated with CytB and it appears, from the protein-to-lipid ratio, that the CytB is binding to the external surface of the bilayer. This implies that the irreversible nature of the interaction is not due to the insertion of the pore into the hydrophobic interior of the bilayer and is in agreement with observations that the initial association of the CytB with membranes is irreversible.¹²

Adsorption of proteins to surfaces can have an apparent irreversibility with a kinetic origin due to multiple attachments. In addition to this, there are several possible forces that can interact to cause irreversible association of proteins with surfaces.³⁹ These forces include dehydration of the protein or the adsorbent and an increase in the conformational entropy of the polypeptide chain. Dehydration of the lipid headgroups as the protein interacts with the external surface of the lipid layer is possible. Dehydration of proteins as they adsorb to surfaces will require close contact which typically involves denaturation of the protein and a concomitant increase in rotational freedom. The CytB does not denature on interaction with membranes, although proteolysis studies indicate that there are some conformational changes.¹⁴ Insertion of CytB into a lipid bilayer could well involve dehydration of the protein as the CytB inserts into the hydrophobic portion of the bilayer. Transfer of charged groups into the apolar environment at the interior of the bilayer will decrease the interaction. This leaves dehydration of the lipids and electrostatic interactions at the external surface of the bilayer as the possible driving forces promoting the association of CytB with the external surface of the bilayer and dehydration of the protein as a possible driving force for insertion into the hydrophobic bilayer interior. Analyses based on reversible thermodynamics were not performed here due to the fact that the association is irreversible over the timescale studied.

Cooperativity of CytB Binding. Figure 6 shows that as more aliquots of $20 \mu\text{g mL}^{-1}$ CytB are added to the

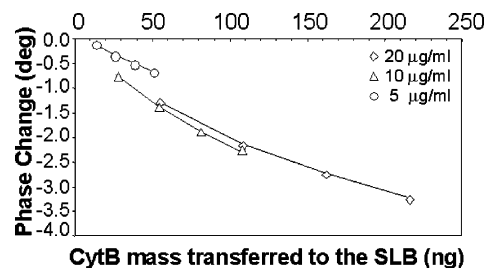


Figure 8. Plot of total phase change as a function of the calculated total CytB mass transferred to the SLB surface (ref 37) during the addition of aliquots of different concentrations.

bilayer, the rate and extent of CytB association decrease. This indicates that the presence of some CytB associated with the bilayer did not facilitate further addition of CytB at this solution concentration and protein-to-lipid ratio. CytB associated with the bilayer would be able to facilitate further additions if there were monomers or partially formed oligomers in association with the membrane and if the CytB monomers in solution had a higher affinity for membrane-associated CytB than for the lipids in the bilayer. If both these conditions were fulfilled, then the bilayer-associated CytB could provide higher affinity binding sites than the bilayers. Figure 6 shows no sign of this happening at any fractional coverage of the bilayer for addition of CytB at $20 \mu\text{g mL}^{-1}$.

One possible explanation for the results shown in Figure 6 is that CytB monomers or incomplete oligomers do not persist in the bilayer, either because the CytB binds as a fully formed oligomer or because the oligomerization is rapid with respect to the initial association step. There is evidence that CytB and the closely related CytA oligomerize in association with membranes,¹³ which lends some weight to the second of these two hypotheses. Figure 6 could also be explained if CytB from solution associated with lipids and oligomerization took place by lateral diffusion of bilayer-associated protein. Taken in conjunction with other data, Figure 6 would therefore suggest that the CytB oligomerizes rapidly after the initial association with the bilayer under the conditions used here.

Figures 7 and 8 show that CytB binding at $5 \mu\text{g mL}^{-1}$ followed a different pattern from that at higher concentrations. Figure 7 shows that association of some CytB with the SLB seems to facilitate further additions of CytB at $5 \mu\text{g mL}^{-1}$, although this is not very clear since the phase changes involved are very small. The difference between addition at $5 \mu\text{g mL}^{-1}$ and additions at higher concentrations is shown more clearly in Figure 8. If the rate of adsorption is directly proportional to solution concentration, as we assume for the irreversible interaction of CytB with the lipid bilayer, then the total amount adsorbed (rate \times time, i.e., kt) will be proportional to the total amount of CytB added in solution (concentration \times time, i.e., $k[\text{CytB}]t$). This relationship would be expected to break down for higher surface concentrations as the interaction becomes limited by the number of available sites. Figure 8 shows that the amount of membrane-associated CytB, as measured by the total phase change, is a function of the total amount of CytB added to the system; this is demonstrated by the superposition of the plots at 10 and $20 \mu\text{g mL}^{-1}$. Addition of CytB at $5 \mu\text{g mL}^{-1}$ does not, however, produce the same pattern; Figure 8 shows that the mass transfer of the same total amount of protein to the interface, calculated as described in the Supporting Information, produces a relatively low amount of bound toxin at solution concentrations of $5 \mu\text{g mL}^{-1}$. This difference is not likely to be due to increased

(38) Butko, K.; Huang, F.; PusztaiCarey, M.; Surewicz, W. K. *Biochemistry* **1996**, *35*, 11355–11360.

(39) Norde, W.; Haynes, C. A. In *Proteins at Interfaces II*; Horbett, T. A., Brash, J. L., Eds.; ACS Symposium Series, Vol. 602; American Chemical Society: Washington, DC, 1995; pp 26–40.

oligomerization in solution at higher protein concentrations, since data on the rate of haemolysis indicate that toxin oligomerization most likely occurs after the toxin molecules are associated with the membrane.^{13b} Another explanation could be related to any unfused vesicles attached to the surface of the bilayer; these vesicles, if present, could bind CytB, possibly producing a different change in phase from that occurring as the CytB interacts with a bilayer. This explanation is, however, not very likely, since addition of a fixed amount of vesicles to the surface of the bilayer would be expected to affect addition of an initial fixed amount of CytB. This is not the case here; the total amount of CytB added over four aliquots at $5 \mu\text{g mL}^{-1}$ is equal to the amount added over two aliquots at $10 \mu\text{g mL}^{-1}$. The total amount of protein added in the first aliquot at $20 \mu\text{g mL}^{-1}$ is equal to the total amount added in the first two aliquots at $10 \mu\text{g mL}^{-1}$, producing the same net change in phase; addition of the same total amount of protein in four aliquots at $5 \mu\text{g mL}^{-1}$ produces a smaller total change in phase. The lower rate of addition of CytB at $5 \mu\text{g mL}^{-1}$ is also apparent in Figure 5.

The CytB could bind as a monomer followed by rapid oligomerization in association with the lipids, with the oligomerization process being dependent on the solution concentration of CytB. This model would account for the relatively low amount of CytB bound at a solution concentration of $5 \mu\text{g mL}^{-1}$ and for the previous observations that CytB binds as a monomer. The CytB concentration required to obtain maximum release of entrapped glucose from vesicles will be dependent on the protein-to-lipid ratio and particle size; increasing the protein concentration until oligomers were formed would not in itself be sufficient to obtain maximum glucose release.

Conclusions

CytB appears to associate irreversibly with the external surface of the supported bilayer. Supported bilayers remain on the surface of the acoustic device even at high protein-to-lipid ratios, implying that the protein does not break the bilayer apart in the manner of a detergent. This supports the model of CytB permeabilizing membranes by formation of oligomeric pores rather than by disruption of the lipid bilayer. The presence of some CytB associated with the bilayer did not generally facilitate further addition of CytB; if the CytB binds as a monomer followed by an oligomerization in association with the bilayer, then these results could be explained if the oligomerization were rapid with respect to the initial binding step. The CytB binding at concentrations of $5 \mu\text{g mL}^{-1}$ is less efficient than at higher concentrations, which could possibly be due to oligomerization occurring at higher solution concentrations of protein. The results presented here are consistent with a model in which the CytB binds as a monomer to the external surface of the bilayer, followed by rapid oligomerization if the solution concentration of protein is sufficiently high.

Acknowledgment. Dr. E. Gizeli acknowledges the financial support of the Biotechnology and Biological Sciences Research Council (BBSRC).

Supporting Information Available: Calculation of the CytB mass transfer coefficient. This material is available free of charge via the Internet at <http://pubs.acs.org>.

LA035469X